Unexplained high sensitivity of the reflectance of porous natural photonic structures to the presence of gases and vapours in the atmosphere

Mouchet, S.; Deparis, O.; Vigneron, J.-P.

Published in:
Proc. of SPIE

DOI:
10.1117/12.921784

Publication date:
2012

Document Version
Peer reviewed version

Unexplained high sensitivity of the reflectance of porous natural photonic structures to the presence of gases and vapours in the atmosphere

S. Mouchet, O. Deparis, J.-P. Vigneron

Solid-State Physics Laboratory, Facultés Universitaires Notre-Dame de la Paix (FUNDP), 61, rue de Bruxelles, B-5000, Namur, Belgium.

ABSTRACT

Structurally coloured natural photonic crystals found in several insects are made of ordered porous chitin structures. In such photonic crystals, colour changes can be induced by relative gas/vapour concentration variations in a mixed atmosphere. For instance, when the composition of the atmosphere changes, the colour of *Morpho sulkowskyi* butterfly is modified. Based on this effect, it is possible to identify closely related gases/vapours. In spite of increasing interests for such sensors, the fundamental mechanisms at the origin of the selective optical response are still not well understood. The point is that refractive index variations resulting from the introduction of a specific gas species in the atmosphere are too small to justify the dramatic changes observed in the optical response. Here, we demonstrate through numerical simulations that indeed gas/vapour-induced refractive index changes are too small to produce a significant modification of the spectral reflectance in a representative 3D periodic model of natural porous nanostructures. For this purpose, we used the rigorous coupled wave analysis (RCWA) method for modelling light scattering from inhomogeneous optical media. The origin of the reported colour changes has therefore to be found in modifications of the porous material and their impact on the photonic response.

Keywords: Butterfly wing, natural photonic crystal, structural colour, nanoarchitecture, bioinspiration, selective gas/vapour sensor, reflectance spectra, Bruggeman effective medium

1. INTRODUCTION

In nature, many animals including amphibians, insects and aquatic animals display astonishing coloration effects.[1] Vision and colour play an important role in communication for the living world. They are used indeed in conspecific recognition, in sexual communication, in camouflage or for warning potential predators. Since they influence chances of survival and reproduction, they are subject to strong evolutionary pressure.

There are two origins of coloration: pigmentary colours produced by the selective absorption of light by a pigment, and structural colours produced by the interaction of light with physical nanostructures. In the biological world, colours may originate from one of these two mechanisms or both.

Nanoarchitectures called photonic crystals belong to the second category. They have been existing on our planet for more than 500 million years, not only in the mineral world, as opals, but also in the living world from aquatic animals to butterflies and birds. These are composite materials made of a periodic distribution of media with distinct optical properties, i.e., refractive indexes. The interaction with electromagnetic radiation is selective. The relative contrast between the refractive indexes is at the origin of a photonic band gap. It consists of a well-defined frequency range in which light cannot propagate through the structure. Light with frequencies in the forbidden gap is completely reflected by the structure. These architectures are also called photonic band gap materials, especially when they are not regular but quasiordered. In order to interact with visible light,

Further author information: (Send correspondence to S.M.)
S.M.: email: sebastien.mouchet@fundp.ac.be; phone: +32 (0)81 724701; fax: +32 (0)81 724707
O.D.: email: olivier.deparis@fundp.ac.be; phone: +32 (0)81 725235; fax: +32 (0)81 724707
J.-P.V.: email: jean-pol.vigneron@fundp.ac.be; phone: +32 (0)81 724711; fax: +32 (0)81 724707

Nanophotonics IV, edited by David L. Andrews, Jean-Michel Nunzi, Andreas Ostendorf,
Proc. of SPIE Vol. 8424, 842425 · © 2012 SPIE · CCC code: 0277-786X/12/$18
doi: 10.1117/12.921784

these structures have to meet another condition: their period must be close to the wavelength of visible light, i.e., from tens to hundreds of nanometers.

Butterfly and moth wings are typical examples of such colourful photonic nanoarchitectures.[1] The wing surface is covered by scales having generally the shape of flattened porous scales. The building materials are mainly air and chitin, with a polysaccharide chemical formula $(C_8H_{13}O_5N)_n$. The side of the scale facing the wing membrane is usually unstructured, while the opposite side has longitudinal ridges spaced by about 1 µm, cross-ribs connecting the ridges on a perpendicular way and other elements. The scales are regularly arranged like tiles on a roof. The inner part of the scale is usually made of a complex nanoarchitecture. Two main kinds of nanostructures are found.[1] The first one is the "pepper-pot" structure which is built from perforated layers arranged in a stack. The other one is the "Christmas-tree" geometry. The ridges act as a diffraction grating while the lamellae of the ridges act as multilayer interferometric reflectors. *Morpho* butterflies which are famous for their brilliant iridescent colours,[2] have such nanostructures on their wings.

An amazing property of the coloration of some animals is that they may dynamically change. This phenomenon can be due to different processes: neural control,[3] hormone levels[4] or abiotic factors[5–7] in response to background coloration, breeding condition, reproductive or excitation state. The colour modification is sometimes very rapid. It can occur through the change in pigment or in nanostructure.

In 2007, the modification of coloration and brightness of several structurally coloured butterfly wings induced by the alteration of the surrounding atmosphere was observed.[8] Due to the occurrence of different spatial periodicities in the scale nanostructures from different regions of the wing, butterfly wings could be used as sensors of natural origin being able to fingerprint selectively some gases and vapours. We remind here that vapour is the gaseous form of a substance at a temperature lower than its critical temperature. As well as being perfectly selective, these natural devices were also very sensitive. The smallest detectable fraction was indeed claimed to be 1-2 p.p.m.* Recently, researchers investigated twenty different butterfly and moth species and demonstrated fast, reproducible species-dependent selective sensitivity to seven test vapours.[9] The structures occurring on butterfly wings are open, which makes them capable of fast gas exchange with the surrounding medium and fast sensing, as gases or vapours can easily penetrate in the volume. The high surface to volume ratio also favours the interaction between gases or vapours and the structure, promoting the response.

In spite of increasing interests for such sensors, the fundamental mechanisms at the origin of their selective optical response are still not well understood. Furthermore, this phenomenon is often explained by refractive index variations due to the change of chemical composition of the air filling the pores of the photonic crystals.[10,11] However, refractive index variations Δn resulting from the introduction of a specific gas or vapour species in the surrounding atmosphere (typically $\Delta n \simeq 10^{-6} - 10^{-7}$ between dry air and 50% relative humidity moist air) are too small to justify the dramatic changes observed in the reflectance spectra. In this article, through numerical simulations, the origin of the reported colour changes is demonstrated to arise from modifications of the porous material and their impact on the photonic response. We investigate two phenomena which are supposed to be at the origin of spectral response modifications. The first one is the swelling of the photonic structure and the second one is a combination of surface adsorption at low concentration of gas or vapour species and capillary condensation at high concentration.

The study of these nanoscale structures could be the source of novel various bioinspired systems with similar but optimized functionalities and constitute a kind of "library" of potential sensor nanoarchitectures. Furthermore, it can help us getting better understanding of the photonics of insect scales.

These biodegradable and complex elements cannot easily be synthesized using available technology. However, several fabrication techniques have been developed to replicate these natural photonic structures.[12,13]

The sensing process which can be developed based on optical discrimination of gases/vapours may simplify the current technology based on modulation of electrical properties and reduce the production costs. Indeed, in current sensors, the artificial nanostructures must be chemically modified in order to discriminate different gases/vapours and complicated arrays are used in order to detect closely related gases/vapours. That means that a lot of energy is used in the fabrication of these devices. The biological synthesis, on the other hand, takes

*1 p.p.m. $\equiv 1 \times 10^{-6}$.

place at room temperature and under mild conditions, using C, H, N, O, Ca, Mg atoms and few trace elements. The natural nanoarchitectures occurring in these insects could be the basic elements of very cheap sensors since rearing butterflies is very simple.

2. METHODOLOGY

Potyrailo *et al.*[8] as well as Biró *et al.*[9] highlighted coloration modifications in response to changes in the surrounding atmosphere by measuring reflectance spectra. In our theoretical study, we simulated reflectance spectra of different photonic structures by using the rigorous coupled wave analysis (RCWA) method for modelling light scattering from inhomogeneous optical media.[14] This method was relevant in our case because diffracting photonic models were used. However, due to the model pore size and interdistance, diffraction effects were found to be weak for both structure models discussed below. Our calculations included multiple scattering effects and enabled us to determine the total reflectance from a photonic crystal film according to the incident wavelength, the polar and azimuthal incidence angles and the polarization of the incident wave. We calculated total reflectance spectra using unpolarized visible light at an arbitrary 45°-incident angle. We used at least 8×8 plane waves for the Fourier series expansion of the spatially varying dielectric constant.

2.1 Photonic structure models

A lot of butterflies in which the scales contain pepper-pot type structures, i.e., perforated multilayers, were demonstrated to display colour changes due to surrounding atmosphere variations.[9] It is the case of several Lycaenidae butterflies but also of one moth of the Uraniidae family. Different levels of order characterize this kind of nanoarchitectures, ranging from a fully amorphous structure such as *Pseudolycaena marsyas*[15] to a nearly perfectly ordered photonic crystal, like in *Cyanophrys remus*.[16]

In our study, we simulated the optical response of two different structure models. The first one is a quite simple pepper-pot structure consisting in a cubic lattice of cubic holes (Fig. 1a). The 1 µm-thick multilayer is composed of two kinds of alternating layers: one is homogeneous, only made of bulk chitin which refractive index is $n = 1.56$,[17] and the other one is inhomogeneous, made of porous chitin. These two layers are both 100 nm-thick. The entire multilayer is formed of five such bilayers (Fig. 1a). The pores which are filled with air are defined as cubes. Although the cubic morphology of the holes is unlikely to be found in butterfly wings, its dimensions are compatible with electron microscopy observations of lycaenid butterfly species.[18,19] In fact, the shape of the holes does not really matter since their dimensions are small compared to the wavelength of light.

In order to get closer to realistic architectures, a second structure model was studied. This model was inspired from the inverted opal photonic crystal found in the ventral scales of the southeastern Brazilian butterfly *Cyanophrys remus* (Hewitson, 1868). Colour variations due to a modification of the ambient air were observed for those lycaenid butterfly wings.[9] They were previously investigated morphologically and optically by Kertész *et al.*[16] For our computations, we assumed a photonic film made of a stack of three such unit cells in the vertical direction (Fig. 1b). The dimensions of the *fcc* inverse opal model were compatible with descriptions by Kertész *et al.*[16] The cubic lattice parameter was $d = 395\,\text{nm}$. The distance between neighbouring air spheres was therefore equal to $a = \frac{d}{\sqrt{2}} = 279\,\text{nm}$. The filling factor was $p_{air} = 4\frac{\frac{4\pi R^3}{3}}{d^3} = 0.43$ (R: sphere radius). The Miller indices of the crystal direction we selected were [111].

For both photonic structure models, the incident medium and the substrate were assumed to be made of air and chitin, respectively.

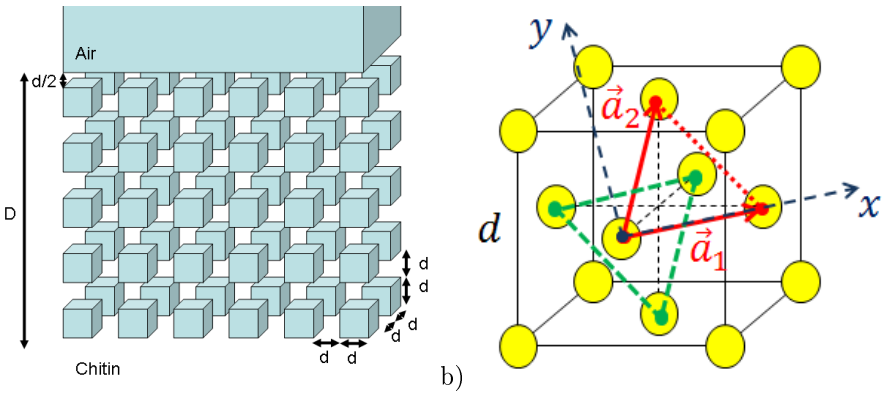

Figure 1. a) First structure model consisting in a cubic lattice of cubic holes with a edge length of $d = 100\,\text{nm}$. The multilayer thickness D is 1 µm. Note that it is an inverted illustration: the air is represented in blue (colours available online) while chitin is not represented and appears transparent in order to highlight the air pores. b) Second structure model consisting in an inverse opal photonic crystal made of air and chitin. The cubic lattice parameter is equal to $d = 395\,\text{nm}$ and the norm of the triangular lattice vectors $\vec{a}_1$ and $\vec{a}_2$ is $a = 279\,\text{nm}$.

In both models, air cavities are not connected with the outside. This property is of course needed in order to allow coloration changes induced by atmosphere concentration variations. Since pore interconnections such as narrow channels, would not influence significantly the photonic response of the structures, they were neglected in our computations in spite of the fact that the pepper-pot structures in the scales of butterfly wings are actually open.

2.2 Gas/vapour refractive indexes

The gases and vapours we used in our simulations were dry air, moist air with different relative humidities ($R.H.$) and ammonia (NH_3). Colour modifications of butterfly wings due to these gases and vapours were experimentally demonstrated.[8,9] It would be relevant to study also other gases and vapours used for these experiments - one can indeed wonder what is the interest to detect optically a gas such as ammonia which is easily detected by the human sense of smell. Unfortunately, it was not possible to find the values of refractive indexes according to the wavelength with a sufficient accuracy for other gases or vapours. A knowledge of the dependence of the refractive index on the wavelength is required. Since the difference in refractive index Δn is, for instance, $\Delta n \simeq 10^{-6} - 10^{-7}$ between dry air and 50% relative humidity moist air and since the refractive indexes of the studied gases and vapours vary by $\delta n \simeq 10^{-5}$ when the light wavelength varies from 350 nm to 700 nm, we can easily understand the importance to take the wavelength dependence into account with a sufficient accuracy.

An update of the Edlén equation for the refractive index of air[20–22] enabled us to calculate the refractive index of dry air n_{TP} at temperature T [°C] and pressure P [Pa]:

$$n_{TP} - 1 = (n_s - 1) \times \frac{P\left[1 + P\left(60.1 - 0.972T\right) \times 10^{-10}\right]}{96095.43\left(1 + 0.003661T\right)}, \tag{1}$$

where n_s is the refractive index of dry air at 15°C and 101325 Pa and is given by the dispersion equation:

$$(n_s - 1) \times 10^8 = 8342.54 + 2406147\left(103 - \sigma^2\right)^{-1} + 15998\left(38.9 - \sigma^2\right)^{-1}, \tag{2}$$

with $\sigma^{-1} = \frac{1}{\lambda_{vac}}$ and λ_{vac} [µm] is the wavelength of electromagnetic radiation in vacuum.

The refractive index of moist air n_{TPp} with a partial pressure p [Pa] of water vapour at total pressure P and temperature T is given by:

$$n_{TPp} - n_{TP} = -p\left(3.7345 - 0.0401\sigma^2\right) \times 10^{-10}. \tag{3}$$

The relative humidity $R.H.$ corresponding to a partial pressure p is calculated by:

$$R.H. = \frac{p}{P_s(T)} \times 100\%, \tag{4}$$

where p is the partial pressure of the water vapour and P_s is the saturation vapour pressure. The latter can be calculated thanks to the Clausius-Clapeyron relation:

$$\ln\left(\frac{P_s}{P}\right) = \frac{ML_V}{R}\left(\frac{1}{T_0} - \frac{1}{T}\right), \tag{5}$$

where P is, in our case, the atmospheric pressure ($P = 101325\,\mathrm{Pa}$), M is the molar mass of the substance, here water ($M = 0.018\,\mathrm{kg/mol}$), L_V is the vaporisation latent heat ($L_V = 2.26 \times 10^6\,\mathrm{J/kg}$), $R = N_A k = 8.31447\,\mathrm{J/K/mol}$ is the gas constant, T_0 is the boiling temperature of the substance at the given P pressure ($T_0 = 373.15\,\mathrm{K}$) and T is the temperature in K.

For our simulations, the selected relative humidities were equal to 0%, 2%, 4%, 7%, 10%, 15%, 20% and 50%.

The refractive index values of ammonia were calculated by a polynomial regression of experimental data found in a handbook[23] at temperature $T = 273\,\mathrm{K}$ and pressure $P = 101325\,\mathrm{Pa}$. These conditions were also chosen for our computations involving air and moist air.

2.3 Chromaticity diagram

It is important to remember that the description of a colour cannot be limited to its spectral content. Since the studied materials could have applications for the human vision, it is required to take into account the human perception of colours - in spite of the perfection of the human eye, everyone does not perceive the same colour - and the light source - for instance, objects illuminated by street lamps in the night are not perceived the same way as in the daylight. Because of these reasons, it is crucial to measure quantitatively colours in an objective manner. For this purpose, we used the chromaticity diagram defined by the *Commission Internationale de l'Eclairage* (CIE) in 1931, following a procedure described elsewhere.[24]

The visual aspect of a colour is quantified thanks to chromaticity coordinates (X, Y, Z), which are calculated from the reflectance spectrum $R(\lambda)$ using the following relations:

$$\begin{array}{l} X = k \int R(\lambda)\, L(\lambda)\, \overline{x}(\lambda)\, d\lambda \\ Y = k \int R(\lambda)\, L(\lambda)\, \overline{y}(\lambda)\, d\lambda \\ Z = k \int R(\lambda)\, L(\lambda)\, \overline{z}(\lambda)\, d\lambda \end{array}, \tag{6}$$

where k is a normalisation constant such that $X + Y + Z = 1$, $L(\lambda)$ is the light source spectrum, $\overline{x}(\lambda)$, $\overline{y}(\lambda)$ and $\overline{z}(\lambda)$ are colour matching functions defined by CIE[†]. The domain of integration is the visible part of the electromagnetic spectrum. In our computations, the source spectrum was supposed to be the D_{65} illuminant. It corresponds to the average daylight emitted by the sun (supposed to be a 6500 K black body) and received in Northern Europe.[25,26]

The two independent coordinates (X, Y) determines the chromaticity of a given colour in the 2-degree observer chromaticity diagram. We must note that this diagram can only be used for the characterisation of colours as perceived by human eyes but not by other animals.

3. RESULTS AND DISCUSSION

3.1 Prediction

Reflectance spectra were first calculated for both photonic models in dry air and in different atmospheres, assuming wavelength-independent differences of refractive indexes (Fig. 2a and c). The objective was to determine a minimal refractive index variation Δn (with respect to dry air) giving rise to significant reflectance spectral modifications. The differences $\Delta R = R_{air} - R_{\Delta n}$ were therefore calculated (Fig. 2b and d). For the first model (cubic lattice of cubic holes), a refractive index variation of $\Delta n = 10^{-3}$ induced a change in reflectance ΔR lower

[†]http://www.cie.co.at/

than 0.1% which is quite below the lowest measured modification $\Delta R \simeq 6\%$.[9] Even a difference of $\Delta n = 10^{-2}$ changed the reflectance by less than 1%. With $\Delta n = 10^{-1}$, however a significant modification of the reflectance was obtained. For the second model (fcc inverted opal), a variation of refractive index $\Delta n = 10^{-3}$ induced a difference of reflectance $\Delta R < 1.6\%$. Significant reflectance differences were reached with $\Delta n = 10^{-2}$ and $\Delta n = 10^{-1}$.

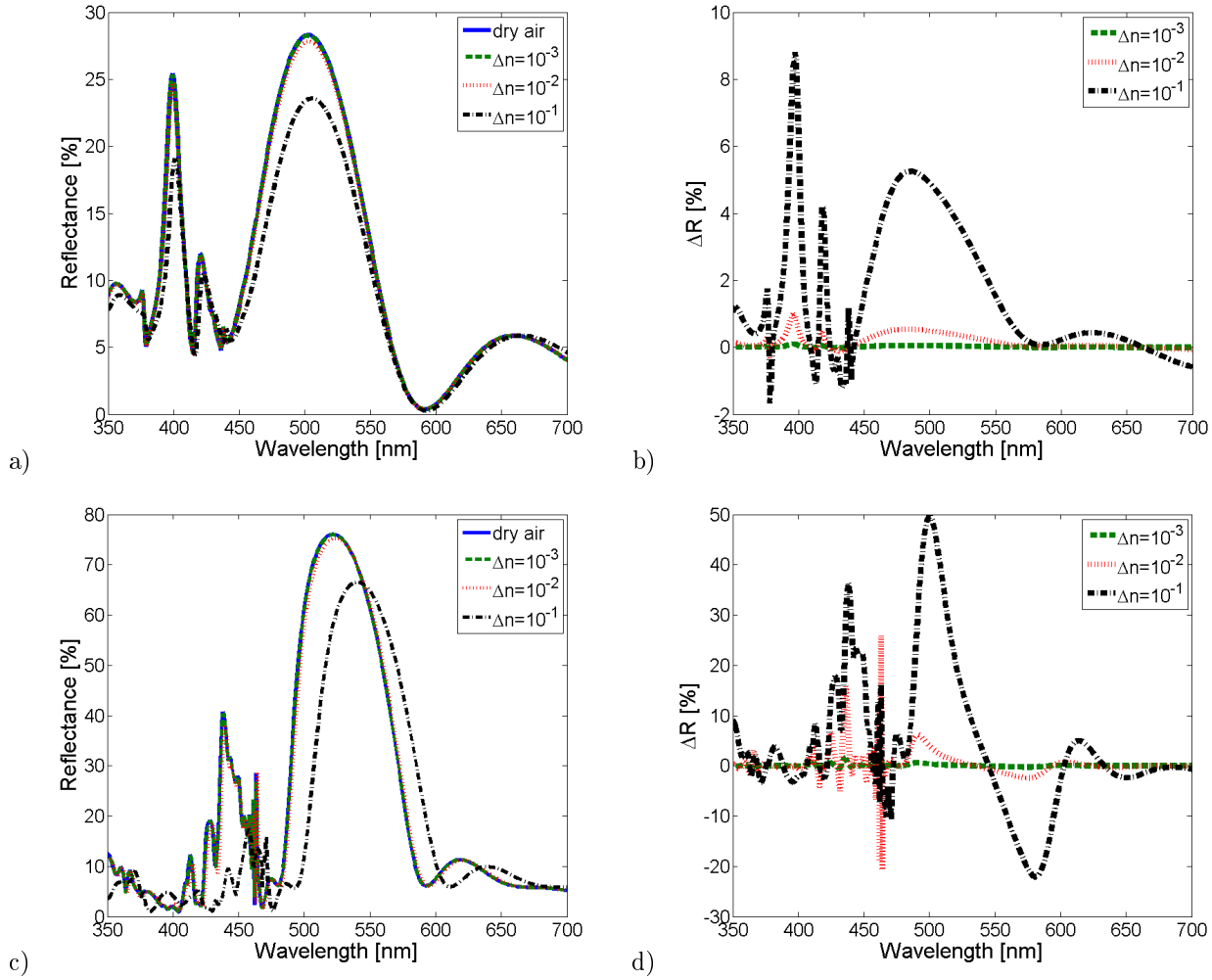

Figure 2. a) Calculated unpolarized reflectance spectra for the first structure model in dry air and in atmospheres having wavelength-independent variations of refractive index $\Delta n = 10^{-3}$, 10^{-2} and 10^{-1}. The spectra corresponding to dry air and $\Delta n = 10^{-3}$ are superimposed. b) Differences ΔR between the reflectance spectrum in dry air and the other spectra plotted in (a). c) Calculated unpolarized reflectance spectra for the second structure model in dry air and in atmospheres having wavelength-independent variations of refractive index $\Delta n = 10^{-3}$, 10^{-2} and 10^{-1}. The spectra corresponding to dry air and $\Delta n = 10^{-3}$ are superimposed. d) Differences ΔR between the reflectance spectrum in dry air and the other spectra plotted in (c).

3.2 Refractive index variation

The reflectance spectra corresponding to the first structure model in selected atmospheres (air, moist air with varying relative humidities ($R.H.$) and ammonia) were then calculated using the available refractive index dispersion laws. They are all nearly identical and reach a maximum at 502 nm. The differences ΔR between the reflectance spectrum in dry air and the other spectra are indeed very tiny. The variation is less than $10^{-2}\%$ between dry air ($R.H. = 0\%$) and an atmosphere only composed of ammonia. The difference of reflectance between

dry air and moist air ($R.H. = 50\%$) is less than $1.5 \times 10^{-5}\%$. Chromaticity coordinates (X, Y) corresponding to the calculated spectra are all superimposed on a single point (0.175, 0.379) in the diagram whatever the studied surrounding atmosphere is (Fig. 3). It corresponds to a bluish green coloration.

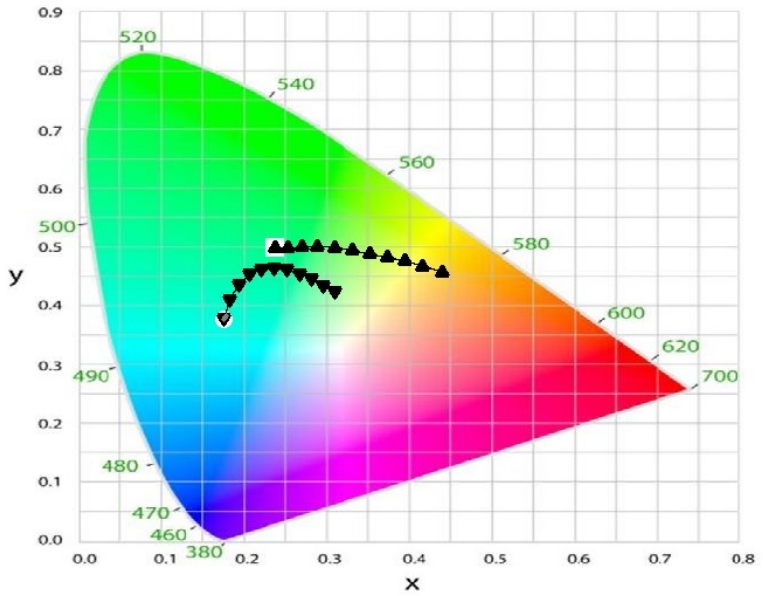

Figure 3. Chromaticity coordinates (colours available online) calculated from the simulated spectra. White circles correspond to reflectance spectra of the first structure model in different atmospheres (air, moist air with varying relative humidities ($R.H.$) and ammonia). All dots are superimposed. White squares correspond to reflectance spectra of the second structure model in different atmospheres. All dots are also superimposed. Black upside down triangles correspond to the evolution of chromaticity coordinates as the first model swells. Black triangles correspond to the swelling of the second model. Grey dots correspond to condensation of water vapour on the inner surface of the pores of the first model.

The reflectance spectra corresponding to the second model were calculated for the same atmosphere conditions. As for the previous results, the spectra are perfectly superimposed, peaking around 522 nm. This value is in accordance with the experimental and computational results obtained by Kertész *et al.*[16] The difference ΔR between dry air and ammonia is here a bit greater, i.e., 0.15%. However, when we only consider water vapour in air, this variation falls down to $10^{-4}\%$. The coloration was evaluated quantitatively by calculating the chromaticity coordinates for these different atmospheres (Fig. 3). The same (X, Y) values are obtained for all spectra, i.e., (0.238, 0.499), located in the green area of the chromaticity diagram.

These results are not surprising since the refractive index variations Δn between dry air and the selected atmospheres are lower than the refractive index difference which is required to modify subtantially the reflectance (cf. previous section): for moist air, $\Delta n < 2 \times 10^{-7}$ (Fig. 4) and for ammonia, $\Delta n < 10^{-4}$.

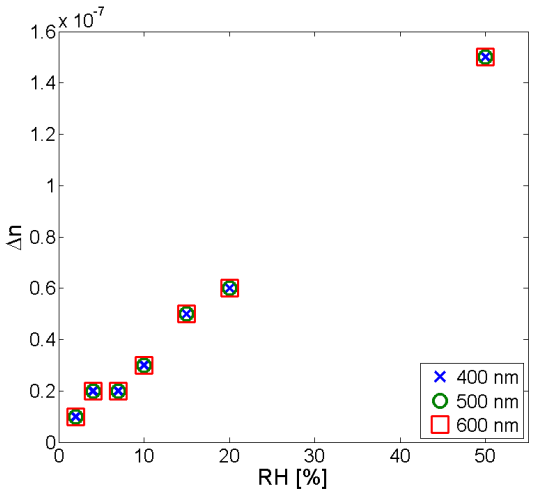

Figure 4. Refractive index variation Δn as a function of the relative humidity $R.H.$ at different wavelengths.

For both structures, the above results allow us to conclude that the colour modification of butterfly wings is not due to the refractive index variation induced by a change in the air composition. This conclusion contrasts with previously reported arguments for explaining colour change in butterfly wings exposed to gas/vapour atmospheres.

Interrestingly, Gao *et al.*[10] derived the optical reflection efficiency with respect to the refractive index of the ambient atmosphere. The results were then applied to a bioinspired grating model mimicking the nanostructure located on the scales of the wing of *Morpho didius*. Their observations are quantitatively close to those we obtained. However, they concluded that changes in the refractive index led to changes in the reflection spectra while we conclude that these modifications are to small to be perceived by the human eye, as it is demontrated by our calculation of the chromaticity coordinates.

We therefore investigated two other possible phenomena, which could explain the modification of the colour with changes in the air composition. These two processes are 1) the swelling of the photonic structure and 2) the physisorption of vapours on the inner surface of the structure (Fig. 5). In order to study the influence of these mechanisms, we assume that the surrounding atmosphere is moist air with a relative humidity $R.H. = 50\%$.

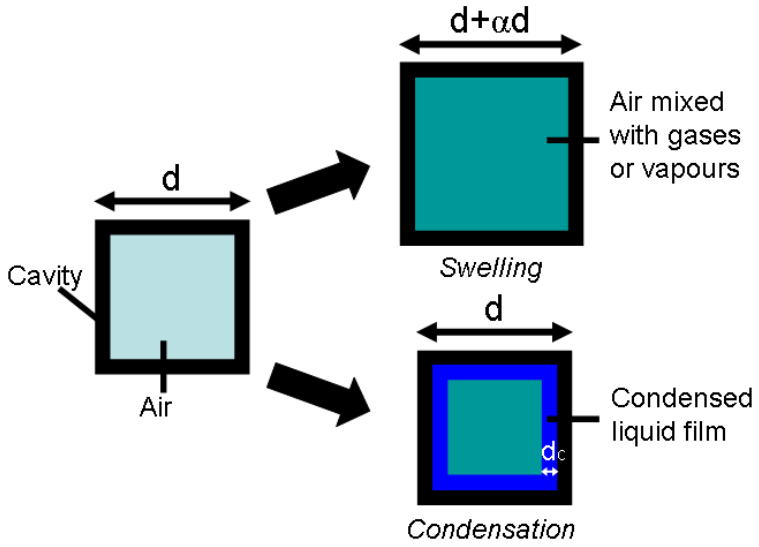

Figure 5. Phenomena explaining possibly the colour modification of butterfly wings when they are exposed to different air compositions. d is the edge length of a cubic pore, α, the swelling factor and d_c, the thickness of condensed liquid film at the inner surface of a cubic pore in the photonic structure. The case of the first structure model (cubic array of cubic holes) is illustrated.

3.3 Swelling

The swelling of the photonic structure is the increase of the structure dimensions and therefore of the spatial periodicity, if any. If the dimensions of the photonic crystal are modified, the reflected light spectrum is also altered.

Swelling of photonic structures were observed in bird feathers, e.g., the bleu-green plumage of tree swallows, *Tachycineta bicolor*,[27] and the pink-violet feathers of mourning doves, *Zenaida macroura*,[28] and in beetle scales located on the elytra of the longhorn beetle *Tmesisternus isabellae*.[7]

There are a lot of other examples of natural materials changing in response to humidity, e.g., plant tissues acting as motors to expel seeds from parent plant and/or to bury them in the soil (seed-bearing pine cones[29] and wheat awns[30]), spider silk[31] in which water infiltration disrupts hydrogen bonding in the amorphous region of proteins, causing a swelling of the silk. Drying, on the other hand, results in contraction of the material. Since all these materials are hydrophilic, changes in the structure dimensions would be caused by impregnation of water.

In the case of tree swallows, the colour changes from blue-green to yellow-green due to the swelling of the keratin cortex from 148 to 158 nm. Regarding the elytra of the longhorn beetle *Tmesisternus isabellae*, the periodicity of the layers structure increases from 175 nm in dry state to 190 nm in wet state. In these two cases, swelling is smaller than 10%. We therefore computed reflectance spectra of photonic structures with a swelling factor α ranging from 0 to 10% (Fig. 6a and c). For both structure models, the same swelling factor α was used. The swelling results in a redshift of the reflectance spectrum in both cases, without noticeable changes in the shape of the spectrum. The peak shifts from 502 nm to 552 nm for the first model and from 522 nm to 574 nm for the second model. Since photonic crystals can often be approximated by a multilayer,[16,32] the redshift of the reflectance spectrum can be predicted by the dominant reflected wavelength formula giving the peak position reflected by a multilayer reflector:

$$\lambda_{dom} = \frac{2a\sqrt{\overline{n}^2 - n_0^2 \sin^2\theta}}{m}, \tag{7}$$

where a is the period of the multilayer, $\overline{n}$ is the average refractive index of the structure, n_0 is the refractive index of the incident medium (in our case, $n_{air} = 1$) and m is an integer such that the dominant reflected wavelength

is in the visible spectrum (m is often equal to 1 for natural structures). If the period a increases, the dominant reflected wavelength λ_{dom} increases too, which explains the observed red shift.

The differences $\Delta R = R_{0\%} - R_\alpha$ between the reflectance spectrum without swelling ($R_{0\%}$) and the other spectra (R_α) is significant - up to about 20% for the first model and up to about 70% in the case of the second model (Fig. 6b and d). In order to evaluate the coloration modification, the evolution of chromaticity coordinates as the stucture swells is plotted on the chromaticity diagram (Fig. 3). The two independent coordinates (X, Y) describe a curve as the structure swells with a factor α increasing from 0 to 10%. Such a curve allows us to figure out the change in the visual aspect of the object. For the first model, the colour is bluish green without swelling, turns green and finally yellowish green as the structure progressively swells. The coloration of the second model is green at the beginning, then, the curve crosses the yellowish green and yellow green areas, before ending in the greenish yellow area.

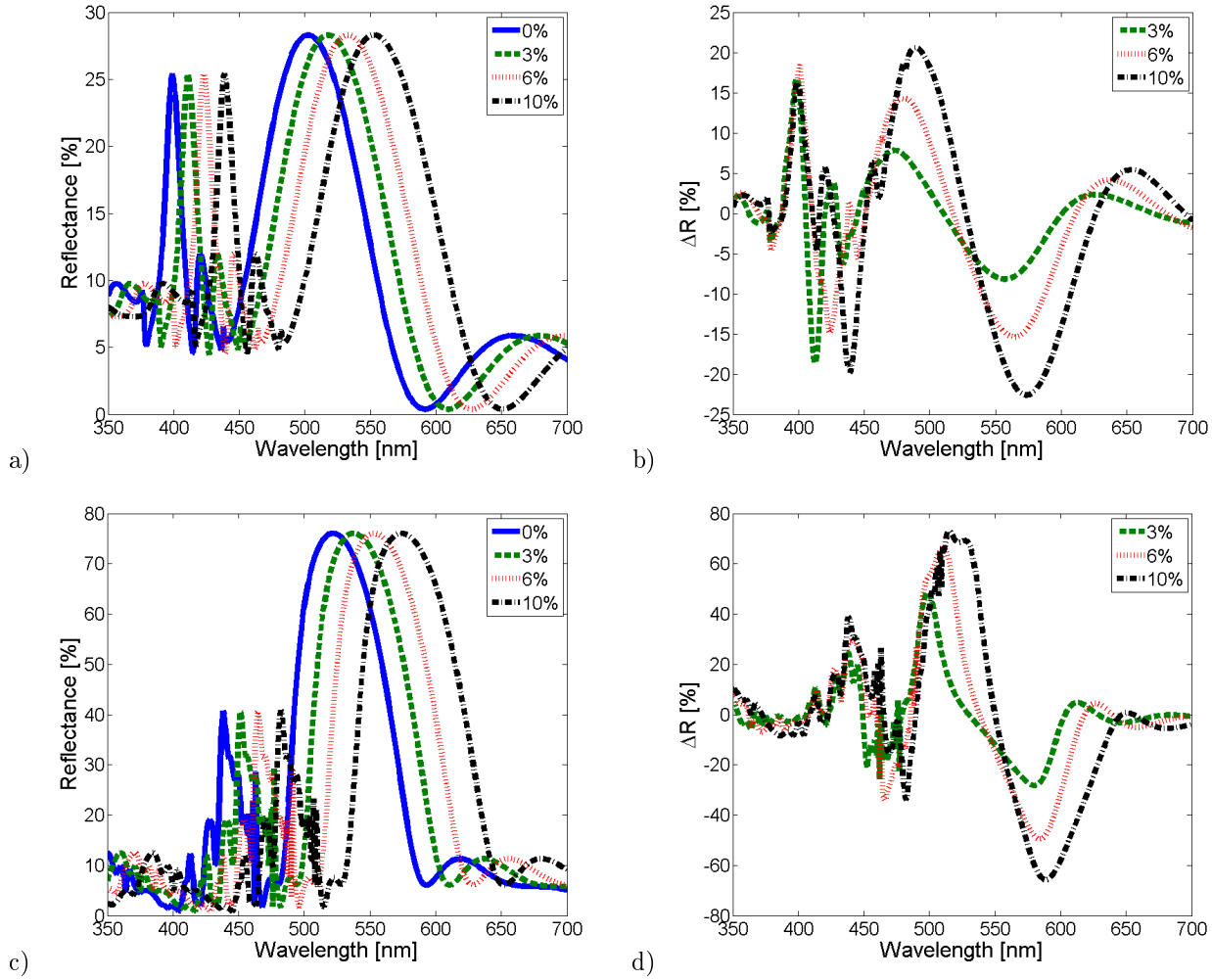

Figure 6. a) Calculated unpolarized reflectance spectra for the first structure model with a swelling factor α ranging from 0 to 10%. b) Differences ΔR between the reflectance spectrum without swelling and the other spectra plotted in (a) c) Calculated unpolarized reflectance spectra for the second structure model with a swelling factor α ranging from 0 to 10%. d) Differences ΔR between the reflectance spectrum without swelling and the other spectra plotted in (d).

3.4 Physical adsorption and capillary condensation

The modification of the spectral response to ambient air may be due to the combination of two mechanisms in the nanosize pores of the butterfly scales, namely physical adsorption - or physisorption - and capillary

condensation of condensable vapours. The curved surface of the pore increases the attraction of wetting substance molecules interacting through van der Waals forces with the material, resulting in surface adsorption and capillary condensation. At low concentrations, gas and vapour molecules are likely to be adsorbed in the pores. At intermediate and high concentrations, the pores are filled rapidly with molecules in liquid state due to capillary condensation. The latter process starts in pores with the smallest radii. Porous silicon based gas sensors actually rely on similar phenomena.[33]

As the air in the pores of the nanostructure is replaced by liquid, the refractive index increases. Indeed, when exposed to vapours, the average refractive index of the porous chitin material changes. Originally, it is lower than for bulk chitin because of the air voids in the material. The higher the porosity, the lower the average refractive index. In the presence of a vapour, capillary condensation reversibly increases the average refractive index, as air ($n_{air} \simeq 1$) is replaced by condensed vapour ($n_{vap} > 1$). Bruggeman's effective medium approximation is an adequate model used to evaluate the refractive index of a porous material. At equilibrium, it assumes that the vapour fills a fraction f of the pore spherical volume according to the equation:

$$(1-p)\,\frac{\varepsilon_{ch}-\varepsilon_{Pch}}{\varepsilon_{ch}+2\varepsilon_{Pch}} + (p-f)\,\frac{\varepsilon_{air}-\varepsilon_{Pch}}{\varepsilon_{air}+2\varepsilon_{Pch}} + f\,\frac{\varepsilon_{vap}-\varepsilon_{Pch}}{\varepsilon_{vap}+2\varepsilon_{Pch}} = 0 \tag{8}$$

where p is the material porosity, ε_{ch} and ε_{air} are the dielectric functions of chitin and air, f is the liquid fraction of the condensed vapour, ε_{vap} is the dielectric function of the condensed vapour and ε_{Pch} is the dielectric function for the porous chitin structure. A transduction mechanism of porous chitin sensors could rely on this change of average refractive index.

In our computations, an adsorbed film of water was supposed to form liquid layers up to 3 nm thick in the cubic pores of the first structure model. This thickness value was observed on the surface of hydrophilic substances such as mica and silicon.[34]

In the present model (Fig. 1a), the porosity p is defined by:

$$p = \frac{d^3}{(2d)^3} = \frac{1}{8}, \tag{9}$$

where d is the edge length of the cubic holes.

The liquid fraction of condensed vapour can be calculated by:

$$f = \frac{d^3-(d-2d_c)^3}{d^3} = 6\frac{d_c}{d} - 12\frac{d_c^2}{d^2} + 8\frac{d_c^3}{d^3}, \tag{10}$$

where d_c is the adsorbed liquid thickness on the inner surface of the pores (Fig. 5).

The variation of the effective refractive index according to the thickness of the adsorbed vapour film d_c (Fig. 7a) was calculated thanks to the Bruggeman's effective medium approximation (Eq. 8). The data are obtained for a value of d_c ranging from 0 to 3 nm, using wavelength-independent refractive indexes of chitin (n_{ch}), air (n_{air}) and water vapour (n_{vap}) equal to 1.56, 1.00 and 1.33, respectively. The relationship is nearly linear and is approximated by a linear regression ($R^2 = 0.9995$):

$$n_{eff} = 0.019 d_c + 1.49. \tag{11}$$

The linear dependence of the effective refractive index on the liquid fraction in the pores is plotted in Fig. 7b and is given by ($R^2 \simeq 1$):

$$n_{eff} = 0.34 f + 1.49. \tag{12}$$

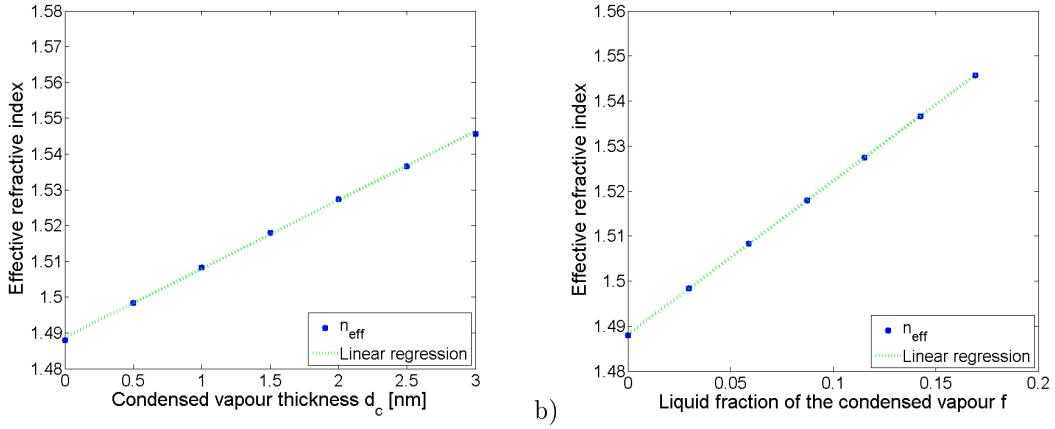

a) b)

Figure 7. Effective refractive index as functions of the condensed vapour thickness d_c (a) and of the liquid fraction of the condensed vapour f (b) calculated by the Bruggeman's effective medium approximation.

The reflectance spectra calculated for a 50% $R.H.$ atmosphere, with an adsorption thickness of liquid water ranging from 0 to 3 nm are shown in Fig. 8a. We can clearly notice a decrease of the reflectance from about 28 to 26% as the quantity of condensed vapour increases, while the peak position slightly shifts from 502 nm to 504 nm. This reduction of reflectance is not surprising. Indeed, infiltration by liquid gives rise to a reduction of the reflectance due to a decrease of the refractive index contrast.[5–7] The differences $\Delta R = R_0 - R_{d_c}$ between the reflectance spectrum without condensation (R_0) and the other spectra (R_{d_c}) are plotted in Fig. 8b. The variations are less important than for the swelling but are certainly detectable. The evolution of the coloration as water vapour condenses is shown on the chromaticity diagram (Fig. 3). The colour modification is not as dramatic as for the swelling. The colour remains in the bluish green area.

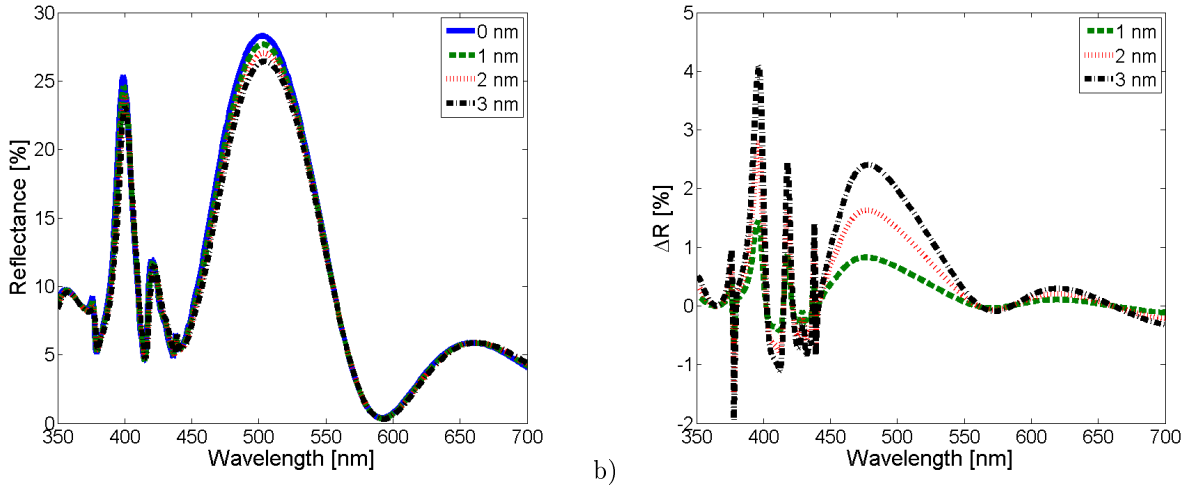

a) b)

Figure 8. a) Calculated unpolarized reflectance spectra for the first structure model with condensation thickness ranging from 0 to 3 nm. b) Differences ΔR between the reflectance spectrum without condensation and the other spectra plotted in (a).

In our simulations, we took only into account pores which could play a role in the interaction of visible light with the structure. Their size was greater than 100 nm, i.e., on the order of visible light wavelength. These pores are therefore classified as a macropores, i.e., pores having a diameter longer than 20 nm. However, it is possible that mesopores (with a diameter between 2 and 20 nm) or micropores (smaller than 2 nm), which does not interact with visible light, are present in these photonic structures and play a role in the effective refractive

index increase as gases or vapours adsorbe into them. They could also play the essential role of interconnecting the macropores in such a way that the porous structure is open to the outside.

4. CONCLUSION

The colour of the scales found on butterfly wings is modified when the air composition is changed. Two main nanostructures are found in the inner part of the butterfly scales: the pepper-pot structure and the Christmas-tree architecture. We demonstrated, by calculating reflectance spectra of pepper-pot structures for different surrounding atmosphere compositions, that the reported coloration modifications cannot be explained by the variation of the refractive index of the atmosphere. This influence cannot be detected by human eyes since no significant modification of the colour is predicted. The origin of the effect is demonstrated to arise from modifications of the porous material. We analyzed two phenomena suspected to be at the origin of coloration modifications: the swelling of the photonic structure and the condensation of water vapour on the inner surface of pores. The swelling of the structure induced a redshift of the reflectance spectra. The shape of the reflectance spectrum was however not modified. A decrease of the reflectance, on the other hand, was caused by the adsorption of water vapour on the surface of pores, while the peak position of the spectra did not change much. Thanks to Bruggeman's effective medium approximation, we analysed the effective refractive index changes according to the condensed liquid quantity in the pores. The relationship between the effective refractive index and the liquid quantity was found to be linear. The coloration variation due to condensation was however rather slight. We therefore conclude that the colour change due to a variation in the surrounding air composition is probably due to one of these two mechanisms influencing the optical response. However, it is very conceivable that a combination of them is at the origin of the phenomenon.

This kind of colour changing behaviour could be an interresting property to exploit in an "intelligent" material. Such materials could lead to the design of novel gas/vapour detection derives. Butterfly wings based or bioinspired sensors could indeed be useful, for example, in food and beverage safety monitoring, moisture level control for exhibition or storage of humidity-sensitive items, in museums, breathalyser or breath analysis.

ACKNOWLEDGMENTS

The authors acknowledge the use of resources of the Interuniversity Scientific Computing Facility (iSCF) located at the University of Namur (FUNDP), Belgium, which is supported by the F.R.S.-FNRS under convention No. 2.4617.07. S.M. was supported as Research Fellow by the Belgian National Fund for Scientific Research (F.R.S.-FNRS).

REFERENCES

[1] Kinoshita, S., [Structural Colors in the Realm of Nature], World Scientific Publishing Co, Singapore (2008).

[2] Berthier, S., [Photonique des Morphos], Springer, Paris (2010).

[3] Mäthger, L. M., Land, M. F., Siebeck, U. E. and Marshall, N. J., "Rapid colour changes in multilayer reflecting stripes in the paradise whiptail *Pentapodus paradiseus*," J. Exp. Biol. 206, 3607-3613 (2003).

[4] Vigneron, J.-P., Pasteels, J. M., Windsor, D. M., Vértesy, Z., Rassart, M., Seldrum, T., Dumont, J., Deparis, O., Lousse, V., Biró, L. P., Ertz, D., and Welch, V. L., "Switchable reflector in the Panamian tortoise beetle *Charidotella egregia* (Chrysomelidae: Cassidinae)," Phys. Rev. E 76, 031907 (2007).

[5] Rassart, M., Colomer, J.-F., Tabarant, T., and Vigneron, J.-P., "Diffractive hygrochromic effect in the cuticle of the hercules beetle *Dynastes hercules*," New J. Phys. 10, 033014 (2008).

[6] Rassart, M., Simonis, P., Bay, A., Deparis, O., and Vigneron, J.-P., "Scales coloration change following water absorption in the beetle *Hoplia coerulea* (Coleoptera)," Phys. Rev. E 80, 031910 (2009).

[7] Liu, F., Dong, B. Q., Liu, X. H., Zheng, Y. M. and Zi, J., "Structural color change in longhorn beetles *Tmesisternus isabellae*," Opt. Express 17(18), 16183-16191 (2009).

[8] Potyrailo, R. A., Ghiradella, H., Vertiatchikh, A., Dovidenko, K., Cournoyer, J. R. and Olson, E., "*Morpho* butterfy wing scales demonstrate highly selective vapour response," Nat. Photonics 1, 123-128 (2007).

[9] Biró, L. P., Kertész, K., Vértesy, Z. and Bálint, Zs., "Photonic nanoarchitectures occurring in butterfly scales as selective gas/vapor sensors," Proc. SPIE 7057, 705706 (2008).

[10] Gao, Y., Xia, Q., Liao, G. and Shi, T., "Sensitivity Analysis of a Bioinspired Refractive Index Based Gas Sensor," J. Bionic. Eng. 8, 323-334 (2011).
[11] Yang, X., Peng, Z., Zuo, H., Shi, T. and Liao, G., "Using hierarchy architecture of *Morpho* butterfly scales for chemical sensing: Experiment and modeling," Sensor Actuat. A-Phys. 167, 367-373 (2011).
[12] Zhu, S., Zhang, D., Chen, Z., Gu, J., Li, W., Jiang, H. and Zhou, G., "A simple and effective approach towards biomimetic replication of photonic structures from butterfly wings," Nanotechnology 20, 315303 (2009).
[13] Song, F., Su, H., Han, J., Zhang, D. and Chen, Z., "Fabrication and good ethanol sensing of biomorphic SnO_2 with architecture hierarchy of butterfly wings," Nanotechnology 20, 495502 (2009).
[14] Deparis, O. and Vigneron, J.P., "Modeling the photonic response of biological nanostructures using the concept of stratified medium: The case of a natural three-dimensional photonic crystal," Mater. Sci. Eng. B-Adv. 169, 12-15 (2010).
[15] Vértesy, Z., Bálint, Zs., Kertész, K., Vigneron, J.-P., Lousse, V. and Biró, L. P., "Wing scale microstructures and nanostructures in butterflies - natural photonic crystal," J. Microsc. 224(1), 108-110 (2006).
[16] Kertész, K., Bálint, Zs., Vértesy, Z., Márk, G. I., Lousse, V. and Vigneron, J.-P., "Gleaming and dull surface textures from photonic-crystal-type nanostructures in the butterfly *Cyanophrys remus*," Phys. Rev. E 74, 021922 (2006).
[17] Sollas, I. B. J., "On the Identification of Chitin by Its Physical Constants," Proc. R. Soc. Lond. B 79, 474-484 (1907).
[18] Wilts, B. D., Leertouwer, H. L. and Stavenga, D. G., "Imaging scatterometry and microspectrophotometry of lycaenid butterfly wing scales with perforated multilayers," J. R. Soc. Interface 6, S185-192 (2009).
[19] Piszter, G., Kertész, K., Vértesy, Z., Bálint, Zs. and Biró, L. P., "Color based discrimination of chitin-air nanocomposites in butterfly scales and their role in conspecific recognition," Anal. Methods 3, 78-83 (2011).
[20] Edlén, B., "The Refractive Index of Air," Metrologia 2(2), 71-80 (1966).
[21] Birch, K. P. and Downs, M. J., "An Updated Edlén Equation for the Refractive Index of Air," Metrologia 30, 115-162 (1993).
[22] Birch, K. P. and Downs, M. J., "Correction to the Updated Edlén Equation for the Refractive Index of Air," Metrologia 31, 315-316 (1994).
[23] Weber, M. J., [Handbook of Optical Materials], CRC Press, Berkeley, California (2003).
[24] Deparis, O., Vandenbem, C., Rassart, M., Welch, V. L., Vigneron, J.-P., "Color-selecting reflectors inspired from biological periodic multilayer structures," Opt. Express 14(8), 3547-3555 (2006).
[25] Judd, D. B. and Wyszecki, G., [Color in Business, Science and Industry], John Wiley & Sons, New York (1975).
[26] Chamberlin, G. J. and Chamberlin, D. G., [Colour: Its Measurement, Computation and Application], Heyden international topics in science, London, (1980).
[27] Eliason, C. H. and Shawkey, M. D., "Rapid, reversible response of iridescent feather color to ambient humidity," Opt. Express 18(20), 21284 (2010).
[28] Shawkey, M. D., D'Alba, L., Wozny, J., Eliason, C., Koop, J. A. H. and Jia, L., "Structural color change following hydration and dehydration of iridescent mourning dove (*Zenaida macroura*) feathers," Zoology 114, 59-68 (2011).
[29] Dawson, C., Vincent, J. F. V. and Rocca, A., "How pine cones open," Nature 390, 668 (1997).
[30] Elbaum, R., Zaltzman, L., Burgert, I. and Fratzl, P., "The Role of Wheat Awns in the Seed Dispersal Unit," Science 316, 884-886 (2007).
[31] Agnarsson, I., Dhinojwala, A., Sahni, V. and Blackledge, T. A., "Spider silk as a novel high performance biomimetic muscle driven by humidity," J. Exp. Biol. 212, 1990-1994 (2009).
[32] Welch, V. L., Lousse, V., Deparis, O., Parker, A. R., Vigneron, J.-P., "Orange reflection from a three-dimensional photonic crystal in the scales of the weevil *Pachyrrhynchus congestus pavonius* (Curculionidae)," Phys. Rev. E 75, 041919 (2007).
[33] Gao, T., Gao, J. and Sailor, M. J., "Tuning the Response and Stability of Thin Film Mesoporous Silicon Vapor Sensors by Surface Modification," Langmuir 18, 9953-9957 (2002).
[34] Beaglehole, D., Christenson, H. K., "Vapor Adsorption on Mica and Silicon: Entropy Effects, Layering, and Surface Forces," J. Phys. Chem. 96, 3395-3403 (1992).